PHYSICAL REVIEW A **74**, 041603(R) (2006)

Bending-wave instability of a vortex ring in a trapped Bose-Einstein condensate

T.-L. Horng,[1] S.-C. Gou,[2] and T.-C. Lin[3]
[1]*Department of Applied Mathematics, Feng Chia University, Taichung 40074, Taiwan*
[2]*Department of Physics, National Changhua University of Education, Changhua 50058, Taiwan*
[3]*Department of Mathematics, National Taiwan University, Taipei 10617, Taiwan*
(Received 31 March 2006; published 18 October 2006)

Using a velocity formula derived by matched asymptotic expansion, we study the dynamics of a vortex ring in an axisymmetric Bose-Einstein condensate in the Thomas-Fermi limit. The trajectory for an axisymmetrically placed and oriented vortex ring shows that it generally precesses in a condensate. The linear instability due to bending waves is investigated both numerically and analytically. General stability boundaries for various perturbed wave numbers are computed. Our analysis suggests that a slightly oblate trap is needed to prevent the vortex ring from becoming unstable.

DOI: 10.1103/PhysRevA.74.041603 PACS number(s): 03.75.Lm, 03.75.Kk, 67.40.Vs

Vortices are fundamental excitations in gases or liquids, characterized by circulation of fluid around a core. Among all vortical structures, vortex rings (VRs) with closed-loop cores are perhaps the most familiar to our daily experience; their compact and persistent nature has fascinated many researchers for a long time [1]. They can be found in various scales in nature, from the well-known smoke rings of cigarettes to the VRs observed in the wakes of aircraft. Remarkably, quantized VRs with cores of angstrom size have been proved to exist when charged particles are accelerated through superfluid helium [2,3]. The recent achievement of quantized vortices in a trapped Bose-Einstein condensate (BEC) [4–6] have suggested the possibility of producing VRs in ultracold atoms. Several schemes for producing VRs in atomic BECs have been put forward [7–12]. In particular, Feder *et al.* [10] have proposed using dynamical instabilities in the condensate to make a dark soliton decay into VRs. Based on this scheme, VRs in a trapped BEC were first realized experimentally by Anderson *et al.* [13].

In fluids, a VR can move along its axis with a self-induced velocity. Despite their solitary nature, VRs are susceptible to azimuthally wavy distortions and these so-called bending waves may be amplified under certain circumstances. The bending-wave instability of classical VRs has been extensively studied in the past few decades, and its inviscid instability was first explored by Widnall *et al.* [14]; it is a short-wave instability, characterized by $k\xi \sim O(1)$, where k is the wave number of the unstable wave and ξ is the size of vortex core. In this Rapid Communication, we examine the bending-wave instability of a VR in a trapped BEC. The vortex dynamics in a superfluid generally resembles that in a normal inviscid fluid even though the circulation is quantized in the superfluid. However, some essential differences remain regarding the bending-wave instability. For example, the core size of a quantized vortex is extremely small in a large BEC [15], where we may assume $\xi \to 0$. Accordingly, $k \to \infty$ under the condition $k\xi \sim O(1)$, and therefore the Widnall instability would never occur in this limiting case. Yet the trapping potential causes vortex stretching, and the bending-wave instability with wavelength comparable to the ring radius may still occur.

To analyze the stability of the VR in a trapped BEC, we use a scheme developed by Svidzinsky and Fetter, which utilizes the quantum analog of Biot-Savart law to determine the local velocity for each element of the vortex [16]. The velocity formula is derived from the time dependent Gross-Pitaevskii equation by the method of matched asymptotic expansions in the Thomas-Fermi (TF) limit. To be specific, we shall consider a trapping potential $V(\mathbf{x}) = m(\omega_\perp^2 r^2 + \omega_z^2 z^2)/2$ in the cylindrical coordinates (r, θ, z), with the aspect ratio defined by $\lambda = \omega_z/\omega_\perp$. The density profile of the condensate is given by $\rho(\mathbf{x}) = \rho_0(1 - r^2/R_\perp^2 - z^2/R_z^2)$ in the TF limit, where $R_\perp = (2\mu/m\omega_\perp^2)^{1/2}$ and $R_z = (2\mu/m\omega_z^2)^{1/2}$ are, respectively, the radial and axial TF radii of the trapped BEC; μ is the chemical potential and $\rho_0 = \mu m/4\pi\hbar^2 a$ is the central particle density. Thus, the velocity of a vortex line element at $\mathbf{x}$ in a nonrotating trap is given by [16]

$$\mathbf{v}(\mathbf{x}) = \Lambda(\xi,\kappa)\left(\kappa\hat{\mathbf{b}} + \frac{\hat{\mathbf{t}} \times \nabla V(\mathbf{x})}{\mu\rho(\mathbf{x})/\rho_0}\right), \tag{1}$$

where $\Lambda(\xi,\kappa) = (-\hbar/2m)\ln(\xi\sqrt{R_\perp^{-2} + \kappa^2/8})$; $\hat{\mathbf{t}}$ is the unit vector tangent to the vortex line at $\mathbf{x}$, and $\hat{\mathbf{b}}$ is the associated binormal unit vector; κ is the curvature of the vortex line at $\mathbf{x}$. Here the vortex is assumed to carry one quantum of circulation.

The first term in the large parentheses of Eq. (1) is from the local induction approximation (LIA), when the vortex is treated as an infinitely thin filament. It says that the motion is self-induced by the local curvature and is heading in the direction of $\hat{\mathbf{b}}$. In fact, the LIA alone ensures that the arc length between any two points on the vortex line remains invariant and thus the vortex is not stretched, which means the bending-wave instability will never happen [17]. Nevertheless, the external potential brings in a stretching force, $\hat{\mathbf{t}} \times \nabla V(\mathbf{x})$, which makes the bending-wave instability possible. Suppose a circular VR of radius r is initially formed axisymmetrically and remains so afterward, so that $\hat{\mathbf{t}} = \mathbf{e}_\theta$, $\kappa\hat{\mathbf{b}} = (1/r)\mathbf{e}_z$. Since $\xi \ll r < R_\perp$, the logarithmic term in $\Lambda(\xi,\kappa)$ is predominated by the numerical factor $\ln\xi$, whose magnitude is large as $\xi \to 0$. Hence $\Lambda(\xi,\kappa)$ varies very

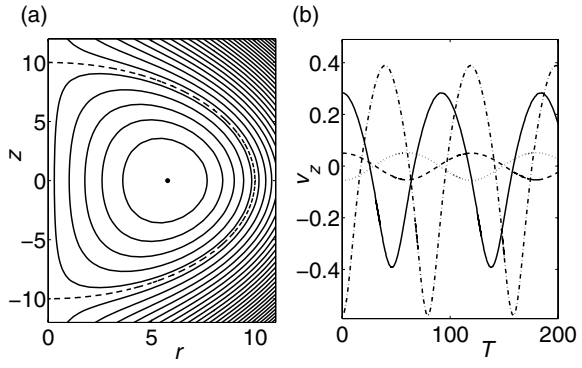

FIG. 1. (a) Phase portrait for Eq. (3) with $\lambda=1$ and $R_\perp=10$. The dashed line indicates the TF limit. (b) Axial velocity $\dot{z}$ (scaled in trap units) as a function of $T=\Lambda t$ for various $r(0)$. The solid, dashed, dotted, and dash-dotted lines represent the cases of $r(0)/r_{\rm eq}=0.5$, 0.9, 1.1, and 1.5, respectively.

slowly with r and we may treat it as a constant. The motion equations then becomes

$$\frac{1}{\Lambda}\dot{r}=\frac{2\lambda^2 z}{G(r,z)},\quad \dot{\theta}=0,\quad \frac{1}{\Lambda}\dot{z}=\frac{-2r}{G(r,z)}+\frac{1}{r},\tag{2}$$

where $G(r,z)=R_\perp^2-r^2-\lambda^2z^2$, and the length, time, and energy are scaled by $(\hbar/m\omega_\perp)^{1/2}$, $\omega_\perp^{-1}$, and $\hbar\omega_\perp$, respectively.

The equation $\dot{\theta}=0$ is redundant. Numerical calculations of the equations of r and z show that the VR moves up and down along z axis cyclically with its radius expanding and shrinking simultaneously. Dividing $\dot{r}$ by $\dot{z}$, we obtain the differential equation relating r and z,

$$\frac{dr}{dz}=\frac{2\lambda^2 rz}{R_\perp^2-3r^2-\lambda^2z^2},\tag{3}$$

of which the solution is $rG(r,z)=C$, where C is a constant. To explore this solution further, we obtain a family of contours with different C's for a given λ, indicating the cyclic motion of the VR as shown in Fig. 1(a) and its associated ring's z component velocity varying with time for several C's in Fig. 1(b). Among all precession solutions, there is a unique stationary solution with $r_{\rm eq}=R_\perp/\sqrt{3}$, $z_{\rm eq}=0$, which is independent of λ and agrees with the result in Ref. [8]. Letting $r_{\rm min}$ and $r_{\rm max}$ be the minimum and maximum values of r for a certain C, we then have $C=r_{\rm min}(R_\perp^2-r_{\rm min}^2)=r_{\rm max}(R_\perp^2-r_{\rm max}^2)$. Integrating the radial equation in Eq. (2) with $r(0)=r_{\rm min}$, $p=(r_{\rm max}^2-r_{\rm min}^2)^{1/2}$, and $q=[r_{\rm max}(2r_{\rm min}+r_{\rm max})]$, we find that r can be expressed in a closed form of t, i.e.,

$$r(t)=\frac{r_{\rm min}r_{\rm max}}{r_{\rm max}{\rm cn}^2\tau+r_{\rm min}{\rm sn}^2\tau}.\tag{4}$$

Here sn $\tau=\tau-(1+k^2)\tau^3/3!+(1+14k^2+k^4)\tau^5/5!+\cdots$ and cn $\tau=1-\tau^2/2!+(1+4k^2)\tau^4/4!+\cdots$ are Jacobian elliptic functions [18], with $\tau=2\Lambda\lambda qt/C$, $k=p/q$.

To study the bending-wave stability of the unperturbed solution given above, let us initialize the coordinates as $r(t)=r_0(t)+\varepsilon r_1(\theta,t)$, $\theta(t)=\theta_0(t)+\varepsilon\theta_1(t)$, and $z(t)=z_0(t)+\varepsilon z_1(\theta,t)$, where εr_1, $\varepsilon\theta_1$, and εz_1 denote the small perturbations with $\varepsilon\ll1$. According to the Seret-Frenet formula $\kappa\hat{\mathbf{b}}=\kappa\hat{\mathbf{t}}\times\hat{\mathbf{n}}=(\partial\mathbf{x}/\partial s)\times(\partial^2\mathbf{x}/\partial s^2)$, where s is the arc length. Currently, it is more suitable to parametrize $\hat{\mathbf{t}}$ and $\hat{\mathbf{b}}$ in terms of θ rather than s. Using the chain rule and the relation $ds=|\partial\mathbf{x}/\partial\theta|d\theta$, it follows that $\hat{\mathbf{t}}=(\partial\mathbf{x}/\partial\theta)|\partial\mathbf{x}/\partial\theta|^{-1}$ and $\kappa\hat{\mathbf{b}}=(\partial\mathbf{x}/\partial\theta)\times(\partial^2\mathbf{x}/\partial\theta^2)|\partial\mathbf{x}/\partial\theta|^{-3}$, and thus, to the linear order of ε, we obtain $\hat{\mathbf{t}}=\varepsilon r_1' r_0^{-1}\mathbf{e}_r+\mathbf{e}_\theta+\varepsilon z_1' r_0^{-1}\mathbf{e}_z$ and $\kappa\hat{\mathbf{b}}=\varepsilon z_1'' r_0^{-2}\mathbf{e}_r-\varepsilon z_1' r_0^{-2}\mathbf{e}_\theta+(r_0-\varepsilon r_1-\varepsilon r_1'')r_0^{-2}\mathbf{e}_z$, where the primed notations indicate the derivatives with respect to θ. Substituting $\hat{\mathbf{t}}$ and $\kappa\hat{\mathbf{b}}$ above into Eq. (1) and expanding all terms in power series of ε, we see that (r_0,θ_0,z_0) satisfy the zeroth-order equations (2). To the first order of ε, we get a set of linearized equations for r_1 and z_1. For further study of the linear stability for bending waves, we express $r_1(\theta,t)=R_1(t)\exp(in\theta)$, $z_1(\theta,t)=Z_1(t)\exp(in\theta)$ where n is an integer. Accordingly, we have

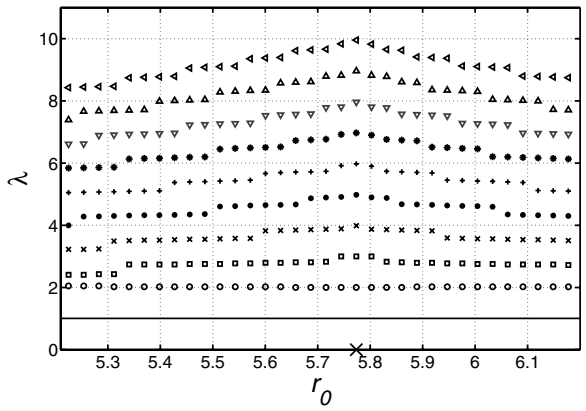

FIG. 2. Stability boundary curves of $|n|=1$ to 10 (from bottom to top) for $R_\perp=10$. The solid line is the stability boundary of $|n|=1$; the circle of $|n|=2$; the square of $|n|=3$, and so forth. For $|n|\neq1$, the region above each boundary curve is unstable for the corresponding mode and stable below. For $|n|=1$, the boundary curve is simply $\lambda=1$; above this it is stable and below it (including it) unstable. The cross on the horizontal axis denotes $r_{\rm eq}$.

$$\frac{\dot{R}_1}{\Lambda}=\frac{-n^2Z_1}{r_0^2}+\frac{2\lambda^2Z_1}{G(r_0,z_0)}+\frac{4\lambda^2z_0(r_0R_1+\lambda^2z_0Z_1)}{G^2(r_0,z_0)},\tag{5}$$

$$\frac{\dot{Z}_1}{\Lambda}=\frac{(n^2-1)R_1}{r_0^2}-\frac{2R_1}{G(r_0,z_0)}-\frac{4r_0(r_0R_1+\lambda^2z_0Z_1)}{G^2(r_0,z_0)}.\tag{6}$$

Here we have ignored the equation of θ_1, which is redundant. In general, $r_0(t)$, $z_0(t)$, $R_1(t)$, and $Z_1(t)$ can only be solved numerically. The linear stability will depend on λ, $|n|$, and $r_0(0)$, by letting $z_0(0)=0$ without loss of generality, and the stability boundaries are shown in Fig. 2. If we focus on the linear stability of a stationary ring, i.e., with $r_0(t)=r_{\rm eq}$, $z_0(t)=z_{\rm eq}$, and further assume $R_1(t)=\alpha\exp(-i\omega t)$, $Z_1(t)=\beta\exp(-i\omega t)$, the condition for nontrivial α and β after substituting the expression above into Eqs. (5) and (6) is given by

$$\det\begin{bmatrix} -i\omega R_\perp^2 & 3\Lambda(n^2-\lambda^2) \\ 3\Lambda(n^2-3) & i\omega R_\perp^2 \end{bmatrix} = 0 \tag{7}$$

From Eq. (7), we obtain the dispersion relation for the disturbance, $\omega_{|n|}(\lambda) = \pm 3\Lambda R_\perp^{-2}[(n^2-\lambda^2)(n^2-3)]^{1/2}$. Obviously, $\omega_{|n|}$ is either purely real or purely imaginary. Real $\omega_{|n|}$ corresponds to a traveling wave with fixed amplitude such that the unperturbed solution is stable. If $\omega_{|n|}$ is otherwise imaginary, with a complex-conjugate pair, such that one of them implies that the amplitude of the bending wave grows exponentially in time, the unperturbed solution is unstable. It is easy to show that when (1) $0 \leq \lambda < 1$, $\omega_{|n|}$ is real for all $|n| \neq 1$; (2) $1 \leq \lambda \leq 2$, $\omega_{|n|}$ is real for all n; (3) $\lambda > 2$, $\omega_{|n|}$ is real for $|n| \leq 1$ or $|n| \geq \lambda$. Hence, we conclude that the ring is absolutely stable when $1 \leq \lambda \leq 2$, for which the BEC is purely spherical to slightly oblate.

The normal mode of the stable wave is given by

$$\begin{bmatrix} r_1^{(n)}(\theta,t) \\ z_1^{(n)}(\theta,t) \end{bmatrix} \propto \begin{bmatrix} 1 \\ \gamma_n \end{bmatrix} e^{i(n\theta-\omega_{|n|}t)} \tag{8}$$

where $\gamma_n = i\omega_{|n|}R_\perp^2/3\Lambda(n^2-\lambda^2)$ is the ratio between α and β for a given $|n|$. The $\pi/2$ phase difference between α and β implies a helical wave along the circumference of the VR. Since $\omega_{|n|}$ always comes in pairs with the same magnitude but opposite sign, there must be two identical helical waves traveling in opposite directions, and the result is a standing wave rotating around the unperturbed core axis, which is named a bending wave. For $n=0$, the rotation is precisely the precession of a circular ring with $r_0(0) \simeq r_{\rm eq}$, and the frequency obtained from the inverse of Eq. (4) by setting $r_{\min} \lessapprox r_{\rm eq} \lessapprox r_{\max}$ is exactly ω_0. The mode with $|n|=1$ is very special. Since the ring is slightly shifted horizontally from its original equilibrium position, it tilts due to the unbalanced force and then wobbles around the xy plane. For $|n| \geq 2$, the bending wave looks like a petal.

The normal mode for the unstable wave is obtained by letting $\omega_{|n|}$ in Eq. (8) be imaginary, when the bending wave, unlike the stable one, is not propagating at all but just grows exponentially in time. The growth of an unstable wave of $|n|=8$ is shown in Fig. 3, where the mode is initially excited and continues to grow for $\lambda = \sqrt{65}$. As the disturbance continues to grow and the vortex ring continues to be stretched, the petal shape becomes more pronounced as shown in Fig. 3(d). The vortex dynamics is catastrophically disrupted when the circumference of the ring diverges. The growth of an unstable wave of $|n|=1$ on a stationary ring is somewhat different from that for other n's and is shown in Fig. 4. In this case, the excited VR wobbles at first as in the stable mode, then gradually turns over, and is seriously distorted at last. In most situations, however, the perturbation is generally random and only the unstable mode with the largest growth rate will be selected to grow and dominate the instability. This most unstable mode is determined by solving $d\omega_{|n|}/dn=0$, and we find that its wave number is closest to $(\lambda^2/2+3/2)^{1/2}$ for $\lambda > 2$. For $0 \leq \lambda < 1$, the only unstable mode is $|n|=1$ with a growth rate $3\Lambda R_\perp^{-2}(2-2\lambda^2)^{1/2}$ which reaches its maximum at $\lambda=0$.

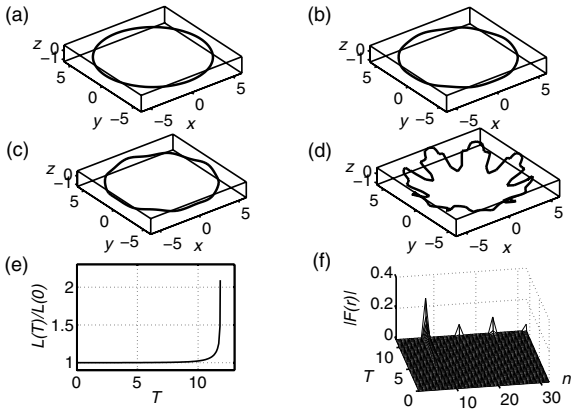

FIG. 3. Growth of unstable waves of $|n|=8$ on a stationary vortex ring at various $T=\Lambda t$, where $\lambda=\sqrt{65}$, $R_\perp=10$. T=(a) 0, (b) 4.90, (c) 7.90, and (d) 11.82. (e) The circumference L of the vortex ring as a function of time. (f) Development of the Fourier components of r. In the long-time limit, the $|n|=8$ mode is most amplified, yet its higher harmonics ($|n|=16$, 24, etc.) are also amplified.

The stability criterion $1 \leq \lambda \leq 2$, where $\lambda = 1, 2$ represents, respectively, the stability boundary for the mode $|n|=1,2$, indicates that a stationary VR is unstable in both cigar- and pancake-shaded BECs. This can be understood as follows. When the BEC is in a cigar shape, as observed in $|n|=1$ mode shown in Fig. 4, the wobbling VR is easier to overturn and gets strongly distorted afterward. When the BEC is in a pancake shape, we can take the $|n|=8$ mode shown in Fig. 3 as an example. The reason that λ must be large enough so as to destabilize this mode can be explained in the following way. For a stationary ring, $\kappa\hat{\mathbf{b}}$ and $\mathbf{F}$ are balanced vectors lying on xy plane, where $\mathbf{F} = \rho_0\hat{\mathbf{t}} \times \nabla V(\mathbf{x})/\mu\rho(\mathbf{x})$ in Eq. (1). When the VR is slightly perturbed, the bending wave rotates around the unperturbed core axis owing to the small imbalance between $\kappa\hat{\mathbf{b}}$ and $\mathbf{F}$ which almost remains on the xy plane. Take any tip of the petal in Fig. 3 as an example. As

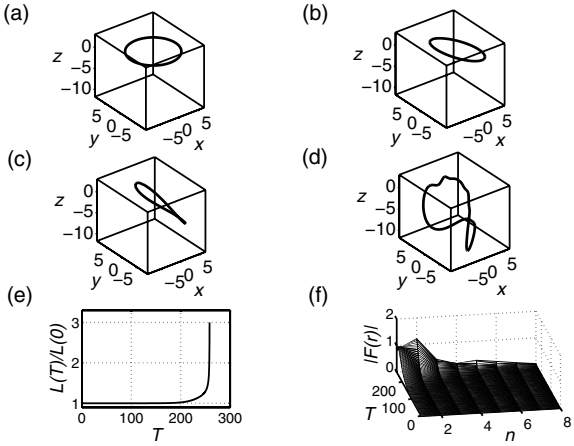

FIG. 4. Growth of unstable waves of $|n|=1$ on a stationary vortex ring at various $T=\Lambda t$, with $\lambda=1/\sqrt{2}$, $R_\perp=10$. T=(a) 0, (b) 200.42, (c) 236.20, and (d) 256.94. (e) The circumference L of the vortex ring as a function of time. (f) Development of the Fourier components of r.

the tip rotates more up from the xy plane, the component of $\mathbf{F}$ in $-\hat{\mathbf{n}}$ direction gets larger chiefly due to $\lambda^2 z$, the z component of ∇V. This $-\hat{\mathbf{n}}$ component acts as a stretching force that will enhance the petal shape if it is large enough. Naturally an instability threshold exists for λ, and $\lambda > 8$ is needed here to destabilize $|n|=8$ mode. As $|n|$ gets larger, so does the curvature κ. Hence, this instability threshold also becomes larger, and this explains the instability criterion $\lambda^2 > n^2$ when $|n| \geq 2$. Unlike the stationary VR, the stability boundary for a precessing VR can only be determined numerically, and the result is shown in Fig. 2. We see that a precessing VR generally has a smaller instability threshold than the stationary one. In addition, the larger the precession trajectory is, the smaller the threshold becomes. This is because the instability of a precessing VR always happens when it is expanding and moving downward, where a larger trajectory would give a smaller $\rho(\mathbf{x})$, and thus increase the magnitude of $\mathbf{F}$.

In summary, we have investigated the dynamics of a single VR and its stability in an axisymmetric BEC in the TF limit. Under axisymmetric initial conditions, the motion equations for the VR are solved analytically. The bending-wave instability follows to be studied and the stability boundaries are computed for various combinations of λ, n, and $r_0(0)$ both numerically and analytically. The main contribution of our studies suggests that the VR can be stable only in a slightly oblate trap.

[1] P. G. Saffman, *Vortex Dynamics* (Cambridge University Press, Cambridge, U.K., 1992).
[2] R. J. Donnelly, *Quantized Vortices in Helium II* (Cambridge University Press, Cambridge, U.K., 1991).
[3] G. W. Rayfield and F. Reif, Phys. Rev. Lett. **11**, 35 (1963).
[4] J. E. Williams and M. J. Holland, Nature (London) **401**, 568 (1999).
[5] M. R. Matthews *et al.*, Phys. Rev. Lett. **83**, 2498 (1999).
[6] K. W. Madison, F. Chevy, W. Wohlleben, and J. Dalibard, Phys. Rev. Lett. **84**, 806 (2000).
[7] B. Jackson, J. F. McCann, and C. S. Adams, Phys. Rev. A **60**, 4882 (1999); T. Winiecki and C. S. Adams, Europhys. Lett. **52**, 257 (2000).
[8] B. Jackson, J. F. McCann, and C. S. Adams, Phys. Rev. A **61**, 013604 (1999).
[9] J. Ruostekoski and J. R. Anglin, Phys. Rev. Lett. **86**, 3934 (2001).
[10] D. L. Feder, M. S. Pindzola, L. A. Collins, B. I. Schneider, and C. W. Clark, Phys. Rev. A **62**, 053606 (2000).
[11] M. Guilleumas, D. M. Jezek, R. Mayol, M. Pi, and M. Barranco, Phys. Rev. A **65**, 053609 (2002).
[12] J. Ruostekoski and Z. Dutton, Phys. Rev. A **72**, 063626 (2005).
[13] B. P. Anderson *et al.*, Phys. Rev. Lett. **86**, 2926 (2001).
[14] S. E. Windnall, D. B. Bliss, and C.-Y. Tsai, J. Fluid Mech. **66**, 35 (1974).
[15] L. Pitaevskii and S. Stringari, *Bose-Einstein Condensation* (Oxford University Press, Oxford, 2003).
[16] A. A. Svidzinsky and A. L. Fetter, Phys. Rev. A **62**, 063617 (2000).
[17] J. S. Marshall, *Inviscid Incompressible Flow* (John Wiley & Sons, New York, 2001).
[18] I. S. Gradshteyn and I. M. Ryzhik, *Table of Integrals, Series and Products* (Academic Press, New York, 1994).